

Collective behavior and spatio-temporal pattern formation in dynamical systems

Thesis summary

Larisa Davidova

December 6, 2017

Collective behavior and pattern formation can arise even in seemingly simple systems. The present thesis provides an insight on the factors that lead to the emergence of self-organization by examining one of the most basic models that demonstrate it, coupled oscillators, and adding complexity to it step by step. Even though the model is theoretical, the discovered trends and transitions explain the difference in the type of synchronization found in equivalent real-world systems, such as metronomes on a common platform versus pendulum clocks attached to a beam. Another model that is studied is a system of economic agents trading wealth on an Erdős-Rényi graph. Performing detailed studies and mapping the parameter space of these systems we uncovered previously unnoticed trends and phase transitions, which can be applied to a variety of real-world problems with similar mechanics.

Contents

1	Introduction	4
1.1	The big picture and motivation of the research	4
1.2	Approach and methodology	4
1.3	Outline of the thesis	5
2	Thesis content	6
2.1	Coupled mechanical oscillators	6
2.2	Multiple non-identical oscillators	9
2.3	Coupled Quantum Mechanical Oscillators	11
2.4	Ruin game on networks	14
2.5	Conclusions	19
3	Scientific contributions	20

1 Introduction

1.1 The big picture and motivation of the research

The topic of spontaneous self-organization is a vast cross-disciplinary area of science which encompasses a large number of research topics. Its applications range from pure mathematics to particle physics or biology, from parallel computing to sociology and psychology. Generally, any time when we are dealing with a system of multiple independent agents or objects that are able to interact with each other, we are talking about self organization.

Spontaneous or emergent self-organization has been known for hundreds of years, mainly from observing simple mechanical systems, such as pendulum clocks. The biggest challenge of studying such type of self-organization is the fact that most of the systems composed of many agents are not analytically solvable and require enormous amounts of computation. That is why this topic has become popular only after the invention of parallel computing.

Today, this field is experiencing an explosion in its popularity in the scientific community due to its complexity and due to the diversity of applications. Whether we want to study the dynamics of a swarm of insects, motion of atoms in a molecule, or synchronization of coupled metronomes, there are common patterns and phase transitions that arise in an emergent manner from the mathematical and physical properties of these systems. The goal of the present thesis is to observe these common patterns and transitions in simple models and investigate which factors they are influenced by.

We start by examining the simplest model that displays spontaneous self-organization, two coupled oscillators on a common substrate. From there on we gradually increase the complexity of the system and take note of new emergent behaviors, while controlling for various parameters and system types. While our findings are purely theoretical, they can be applied to a variety of real-world problems that consist of interacting elements, to find conditions for emergent self-organization, in order to achieve or to avoid such behavior.

1.2 Approach and methodology

The primary instrument of our research is computer simulation. Every system we study is modeled in Mathematica, due to many implemented functions, automatic parallelization, and ease of visualization in this particular software. Equations are solved analytically wherever possible, but more complex non-linear equations are solved numerically.

For systems that simulate a large number of interacting agents, we used the Monte-Carlo and molecular dynamics method.

In order to keep our findings grounded on reality, we compare our simulation results with experimental studies of equivalent systems obtained by other researchers in our group, as well as other researchers from all over the world.

1.3 Outline of the thesis

”Self-organization: general aspects” is the first chapter after a general introduction, and it includes a brief introduction to the topic of self-organization, bifurcation theory, chaos theory, and pattern formation, necessary for understanding the context of the research in the present thesis, as well as an overview of other significant works published in the field.

The chapter ”Coupled mechanical oscillators” starts the main body of the thesis, where we examine a system of two identical oscillators connected to a common platform. We start from an ideal system, and approach reality by adding driving and damping. We compare the obtained results with experimental findings of other research groups that studied systems of metronomes or pendulum clocks.

The ”Multiple non-identical oscillators” chapter further expands on the system of coupled oscillators. What if there are more than two of them on a common platform? What if their natural frequencies vary? We take a look at the theoretical results, as well as an experimental model of metronomes on a rotating platform and find several phase transition points in the parameter space.

The ”Quantum coupled oscillators” chapter takes the oscillator system to the quantum level. Oscillators and the platform are now quantum objects. Although we find that they have a similar behavior to the classical ideal oscillators, there are several differences caused by quantum effects.

The chapter ”Ruin game on networks” changes the subject from oscillators to a multi-agent gambler’s ruin game, where multiple agents, connected by a graph, trade. It is an example of a different type of self-organizing systems, but it also displays pattern formation and phase transitions.

2 Thesis content and main results

2.1 Coupled mechanical oscillators

Spontaneous synchronization was first observed by Christiaan Huygens [1] in 1673, which gave a start to the studies of coupled oscillators. It is an example of a seemingly simple system that can display complex nonlinear behavior. Huygens' experiments have been recently revisited and studied more thoroughly [2] [3], but some mysteries still remained: for example, why do pendulum clocks synchronize only in anti-phase, while other similar systems, like metronomes on a common platform, synchronize in-phase [4]?

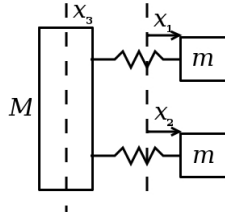


Figure 2.1: *The considered coupled oscillator system.*

To answer this question we start with a generic model of two coupled oscillators connected to a common platform (Fig. 2.1). The Lagrangian for this system is:

$$L = \frac{1}{2}M\dot{x}_3^2 + \frac{1}{2}m(\dot{x}_1 + \dot{x}_3)^2 + \frac{1}{2}m(\dot{x}_2 + \dot{x}_3)^2 - \frac{1}{2}kx_1^2 - \frac{1}{2}kx_2^2, \quad (2.1)$$

where the first term is the kinetic energy of the platform, the second and third terms stands for the kinetic energy of the oscillators relative to the chosen inertial reference frame, and the last two terms are the potential energies of the oscillators. This is a linear system, so we can derive an exact solution to the motion of its parts depending on their initial positions:

$$\begin{aligned} M\ddot{x}_3 &= k(x_1 + x_2) \\ m\ddot{x}_1 &= -kx_1 - m\ddot{x}_3 \\ m\ddot{x}_2 &= -kx_2 - m\ddot{x}_3 \end{aligned} \quad (2.2)$$

After solving these equations for the coordinates, we arrive at the expression for Pearson correlation r depending on initial position a of one of the oscillators, while fixing the other one (plotted in fig. 2.2):

$$r = \frac{\langle x_1 x_2 \rangle_t - \langle x_1 \rangle_t \langle x_2 \rangle_t}{\sqrt{\langle x_1^2 \rangle_t - \langle x_1 \rangle_t^2} \sqrt{\langle x_2^2 \rangle_t - \langle x_2 \rangle_t^2}} = \frac{2a}{a^2 + 1} \quad (2.3)$$

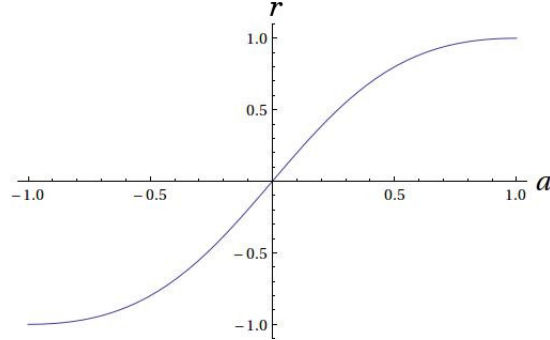


Figure 2.2: *Pearson correlation of the two oscillators coordinate as a function of the initial position of one of the oscillators ($x_1(0) = 1$, $\dot{x}_1(0) = 0$, $\dot{x}_2(0) = 0$ and $x_2(0) = a$, no friction and no driving).*

As expected, this system only displays in-phase synchrony if it starts its motion in synchrony, and anti-phase synchrony if it starts in anti-phase. This type of system cannot display any self-organization, as it lacks an external flow of energy.

In order to make our model display spontaneous synchronization, we can add driving to the oscillators, and friction to both of the oscillators' and the platform's motion. The equations of motion then become:

$$\begin{aligned} M\ddot{x}_3 &= k(x_1 + x_2) + C_1(\dot{x}_1 + \dot{x}_2) - C_0\dot{x}_3 - F_1 - F_2 \\ m\ddot{x}_1 &= -kx_1 - m\ddot{x}_3 - C_1\dot{x}_1 + F_1 \\ m\ddot{x}_2 &= -kx_2 - m\ddot{x}_3 - C_1\dot{x}_2 + F_2 \end{aligned} \quad (2.4)$$

where C_0 is the friction coefficient for the motion of the platform and C_1 is the friction coefficient of the masses on springs, F_1 and F_2 denote the driving forces applied to each of the two masses m . They represent the pulse driving force, which only takes non-zero values when the mass passes its resting position, and acts in the direction of motion of the mass:

$$F_i = P\dot{x}_i\delta(x_i) \quad (2.5)$$

With the introduction of these new parameters and nonlinearity to our original system, it becomes significantly more complex and only solvable numerically. However, after solving it, we notice that the correlation function no longer has a strong dependence on initial positions of the oscillators, but instead demonstrates one of the following behaviors, depending on parameters:

1. complete in-phase synchrony, independent of initial positions
2. complete anti-phase synchrony, independent of initial positions

3. in-phase synchrony for all initial positions $x_2(0) > 0$ and anti-phase synchrony for all initial positions $x_2(0) < 0$
4. stable periodic or quasiperiodic orbit that does not converge to synchrony or anti-synchrony over time

The collective behavior of our initial system did not depend on the masses of the oscillators or the platform, nor on spring constants. However, this time it does. If we fix the masses m and take a look at the parameter space of M and k , we may notice an region of anti-phase synchrony among an overwhelming area of no average synchrony (fig. 2.3), which means there is a certain phase transition from non-synchrony to anti-synchrony that has a linear border.

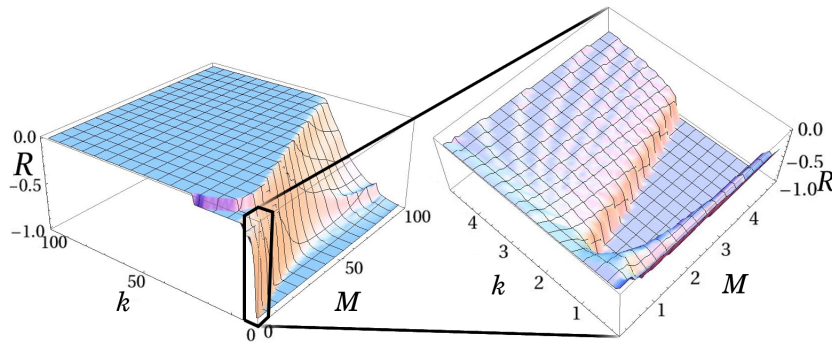


Figure 2.3: *Averaged correlation, R , as a function of M and k . ($C_0 = C_1 = 1$).*

Another part of the parameter space we can take a look at is the friction-driving one. As driving force is compensated by the friction in the oscillators themselves, we can fix one of those values and study only the other. By studying various combinations of friction and mass values, we can see, that there is a very strong phase transition from predominant anti-phase synchrony to mostly in-phase synchrony at $C_1 \approx 9$, independent of any other parameters (fig. 2.4).

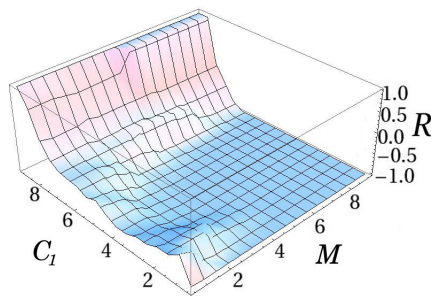


Figure 2.4: *Averaged correlation, R , as a function of M and C_1 . ($C_0 = 1, k = 1$).*

This is the effect that could explain why metronomes always synchronize in-phase, while pendulums only synchronize in anti-phase. Metronomes have higher friction coefficient in their mechanism than pendulums, thus the difference. This is consistent

with other studies on this topic. For instance, Czolczynski, Perlikowski, Stefanski and Kapitaniak, in revisiting Huygens' experiments [3], note the prevalence of anti-phase synchronization in case of identical or near identical pendulums. In another study on identical Huygens pendulums done by Bennett, Schatz, Rockwood and Wiesenfeld [2], the authors also find that these kind of oscillations tend to converge to anti-phase synchrony. In contrast with this, a study by Boda, Neda, Tyukodi and Tunyagi [5] reports only in-phase synchrony for their system of metronomes on a rotating platform.

2.2 Multiple non-identical oscillators

We can expand our model even further by introducing a variable number of oscillators, as well as accounting for the fact that in real-world scenarios the oscillators are non-identical, and have a small variation in their natural frequencies. As the Pearson coefficient is only applicable for calculating the correlation between two variables, and anti-phase synchronization is meaningless when there are more than two parts in the system, we will use the Kuramoto order parameter as a measure of synchrony.

Our goal now is to create a model that is close to the experimental setup of metronomes located on a rotating platform and compare the computational results with the experimental data obtained by Sz. Boda [5].

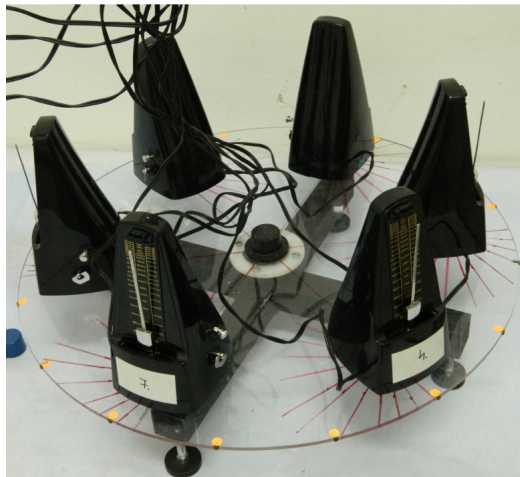


Figure 2.5: *Experimental setup: metronomes are placed on the perimeter of a disc that can rotate around a vertical axis. (Photograph by Sz. Boda)*

As we are not aiming at exact replication of the metronome system, but rather to modify the simple model of masses on springs we used previously, we can just add the extra variables to it, and it should be equivalent to the metronomes. The equations of motion then become:

$$\begin{aligned}
M\ddot{x}_0 &= \sum_{i=1}^N k_i x_i + C_1 \sum_{i=1}^N \dot{x}_i - C_0 \dot{x}_0 - \sum_{i=1}^N F_i \\
m\ddot{x}_i &= -k_i x_i - m\ddot{x}_0 - C_1 \dot{x}_i + F_i
\end{aligned}
\tag{2.6}$$

Unlike in (2.2), this time the number of equations is greater than 2, and $i \in [1, N]$ where N is the total number of oscillators. The variance in natural frequencies of metronomes is accounted for by varying the spring constant k .

Our next step is to determine the values of parameters of our simplified system that will correspond to the real system of metronomes on a platform. By comparing the equations of motion of both systems, we arrive at the following values (see full thesis text for details):

- $m = 0.025\text{kg}$
- $\langle k_i \rangle \in [0.5, 5]\text{kg/s}^2$
- $\Delta k \approx 0.1\text{kg/s}^2$
- $M \in [0.5, 5]\text{kg}$
- $C_1 = 0.0008\text{kg m/s}$
- $C_0 = 0.0001\text{kg m/s}$
- $P = 0.0008\text{kg m/s}$

We assume that there is a number of order-disorder phase transitions that become sharper with increasing number of oscillators. One of these transitions takes place in the M - k parameter space, as soon on fig. 2.6. Its presence is also confirmed by experimental results[6] and the sole reason for its existence is the small difference in the metronomes' frequencies (equivalent to the difference in spring constants in this case), as it does not occur in the case of identical oscillators.

Another such transition takes place as a function of the platform's friction coefficient C_0 (fig. 2.7). Increasing the friction coefficient C_0 effectively reduces the amplitude of the oscillations and weakens the coupling, thus lowering the level of synchronization. Due to the difficulty of controlling precisely the friction coefficient for the platform, there are no experimental studies to compare these findings to.

The presence of these transitions is also confirmed by Ulrichs, Mann, and Parlitz [7], who have done a theoretical study on a similar system of metronomes placed on a movable platform and discovered a sharp spike in the order parameter with the increased coupling strength.

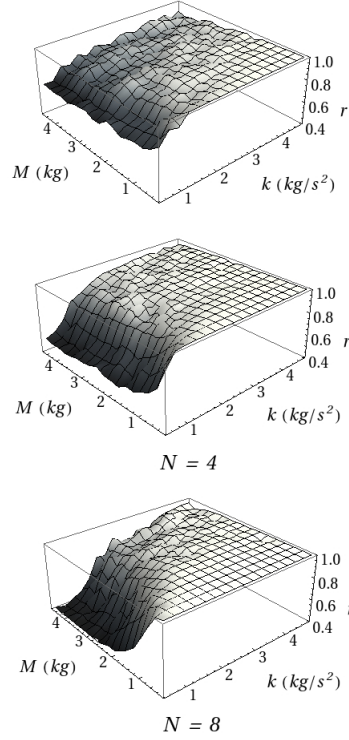


Figure 2.6: The Kuramoto order parameter as a function of the mass of the platform and spring-constants value. Results for different number of oscillators, N , as it is indicated in the figures. ($C_0 = 0.0001 \text{ kg m/s}$)

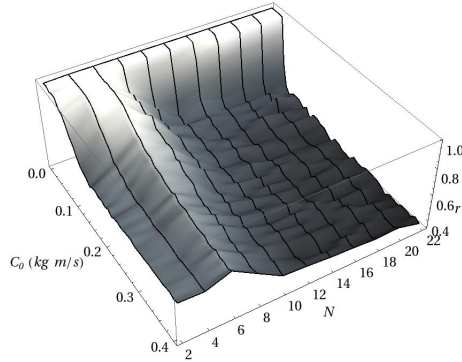


Figure 2.7: The Kuramoto order parameter as a function of the friction coefficient (C_0) of the platform and the number of oscillators on the common platform. ($k = 5 \text{ kg/s}^2$ and $M = 1 \text{ kg}$.)

2.3 Coupled Quantum Mechanical Oscillators

Another fascinating modification of the coupled oscillators model is by shifting to a quantum system, where both the masses and the platform are represented by quantum oscillators and coupling is present. There have been several studies on quantum

oscillators that dissipate heat[8][9], although the topic is relatively new.

The system we study in this chapter is equivalent to the model presented in fig. 2.1, an ideal system without energy dissipation. The Hamiltonian of such system would be:

$$\hat{H} = -\frac{\hbar^2}{2m} \frac{\partial^2}{\partial x_1^2} - \frac{\hbar^2}{2m} \frac{\partial^2}{\partial x_2^2} - \frac{\hbar^2}{2M} \frac{\partial^2}{\partial x_3^2} + \frac{1}{2}k(x_1 - x_3)^2 + \frac{1}{2}k(x_2 - x_3)^2 \quad (2.7)$$

where x_1 and x_2 are the coordinates of the oscillators and x_3 is the coordinate of the platform. We assume that the platform is another quantum oscillator, and in the beginning all three interacting masses start as independent quantum oscillators in their ground states with mean coordinates $\langle x_1 \rangle = x_{01}$, $\langle x_2 \rangle = x_{02}$ and $\langle x_3 \rangle = x_{03}$, respectively. The wave function of such system would be $\Psi_0(x_1, x_2, x_3) = \Psi_{01}(x_1)\Psi_{02}(x_2)\Psi_{03}(x_3)$, where

$$\begin{aligned} \Psi_{01}(x_1) &= \left(\frac{\sqrt{mk}}{\pi\hbar} \right)^{\frac{1}{4}} \exp\left(-\frac{\sqrt{mk}(x_1 - x_{01})^2}{2\hbar} \right) \\ \Psi_{02}(x_2) &= \left(\frac{\sqrt{mk}}{\pi\hbar} \right)^{\frac{1}{4}} \exp\left(-\frac{\sqrt{mk}(x_2 - x_{02})^2}{2\hbar} \right) \\ \Psi_{03}(x_3) &= \left(\frac{\sqrt{Mk}}{\pi\hbar} \right)^{\frac{1}{4}} \exp\left(-\frac{\sqrt{Mk}(x_3 - x_{03})^2}{2\hbar} \right) \end{aligned} \quad (2.8)$$

Our goal is to find the quasi classical trajectories of these oscillators, by calculating the evolution of the wave function and deriving expectation values of coordinates as functions of time:

$$\langle x_i(t) \rangle_{\Psi} = \iiint \Psi^*(x_1, x_2, x_3, t) x_i \Psi(x_1, x_2, x_3, t) dx_1 dx_2 dx_3 \quad (2.9)$$

Then we can find the degree of synchronization via Pearson correlation, same as in eq. 2.3, but with quantum mechanical averaging:

$$r' = \frac{\langle \langle x_1 x_2(t) \rangle_{\Psi} \rangle_t - \langle X_1 \rangle_t \langle X_2 \rangle_t}{\sqrt{\langle \langle x_1^2(t) \rangle_{\Psi} \rangle_t - \langle X_1 \rangle_t^2} \sqrt{\langle \langle x_2^2(t) \rangle_{\Psi} \rangle_t - \langle X_2 \rangle_t^2}}, \quad (2.10)$$

with:

$$\begin{aligned} \langle x_1 x_2(t) \rangle_{\Psi} &= \iiint \Psi^*(x_1, x_2, x_3, t) x_1 x_2 \Psi(x_1, x_2, x_3, t) dx_1 dx_2 dx_3 \\ \langle x_i^2(t) \rangle &= \iiint \Psi^*(x_1, x_2, x_3, t) x_i^2 \Psi(x_1, x_2, x_3, t) dx_1 dx_2 dx_3 \end{aligned} \quad (2.11)$$

In order to do this, we solve the Schrödinger equation numerically on a 3-dimensional grid to obtain eigenvalues and eigenvectors for the Hamiltonian 2.7, after which we can calculate the time evolution of the system.

The resulting trajectories of the oscillator coordinates x_1 and x_2 are similar to the classical trajectories, minus the gradual decrease in amplitude due to the dispersion of the wave function (fig. 2.9).

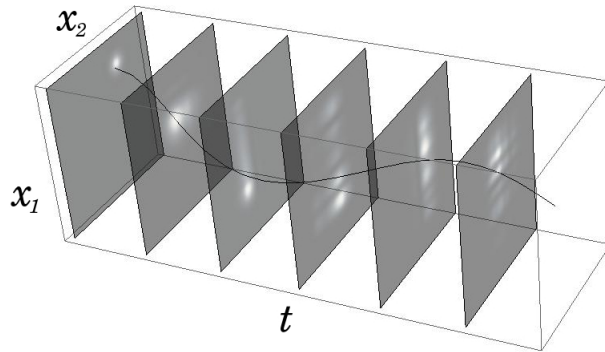


Figure 2.8: *Evolution of the system's wave function in the x_1, x_2 coordinate plane. The line is the trajectory of the expectation value of the system's coordinates.*

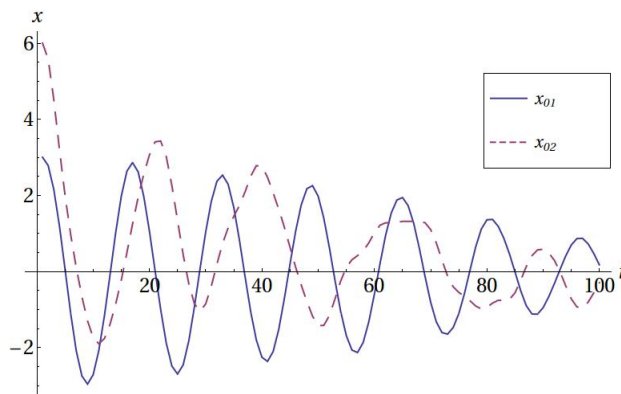


Figure 2.9: *Trajectories of the expectation values of x_1 and x_2 calculated with initial positions $x_{01} = 3$ and $x_{02} = 6$. The decrease in amplitude is due to the dispersion of the wave function.*

The results for correlation, plotted on fig. 2.10, have a few significant differences from the classical case: they depend on the ratio of masses of oscillators and the platform, and they have a sharp transition around origin. It can be speculated that this is due to the fact that in the quantum case the masses aren't point objects, but rather dispersed wave packets, the width of which relative to the oscillation amplitude depends on their masses.

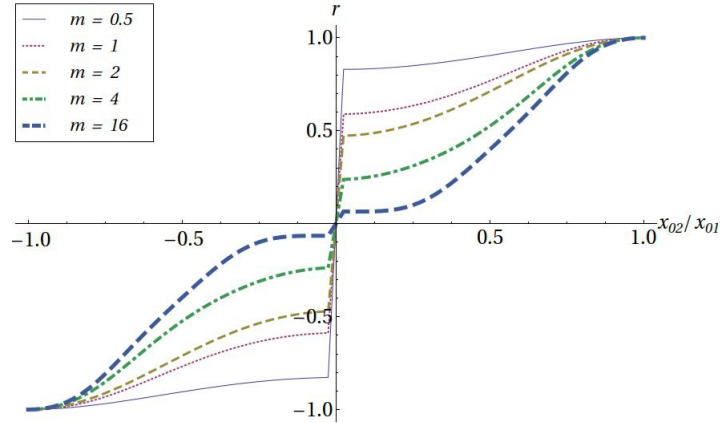


Figure 2.10: *Pearson correlation as a function of the initial position of one of the oscillators. Results for the quantum mechanical system for different m values and $N = 40$.*

2.4 Ruin game on networks

Multiple coupled oscillators is only one example of the many types of systems that display phase transitions and pattern formation. However, pattern formation in this system mainly manifests through temporal patterns, which are defined by the trajectories of the oscillators in time.

We now would like to take a look at another type of system, one that displays spatial patterns. Consider a model of a bidirected random Erdős-Rényi (ER) graph $G(N_0, p)$, defined by the number of nodes, N_0 , and the p probability of having a link between two nodes, where every node is a player. Node degree and average node degree are denoted by k and $\langle k \rangle$ respectively. Each player starts with equal wealth w_0 . The game takes place on a discrete timeline, with equal time intervals as steps. At every step all directly connected nodes on the graph “play” with each other - one player wins a unit of wealth, the other one loses, with the winner and the loser chosen at random. If one of the chosen connected players does not have enough wealth to play, there is no transaction done and we proceed to the next step. The game goes on until there are no more trades possible, i. e. none of the nodes that have non-zero wealth are connected. This model is illustrated in fig. 2.11. Our goal is to predict the average game’s duration and the number of nodes that retain wealth and their wealth distribution until the end as a function of the system’s parameters.

There are two ways to predict the behavior of this system: thermodynamic - dealing with statistics and probabilities, and dynamic, where we study the coarse-grained dynamics of every parameter in the system. Let us start with the thermodynamic, final state approximation.

We assume a fully ergodic approach for the final state of the system, i. e. our main hypothesis is that all allowed configurations are equally probable. This means that we consider the system as micro-canonical. There are several things that limit the final, acceptable configuration: first the remaining nodes cannot be first order neighbors, which

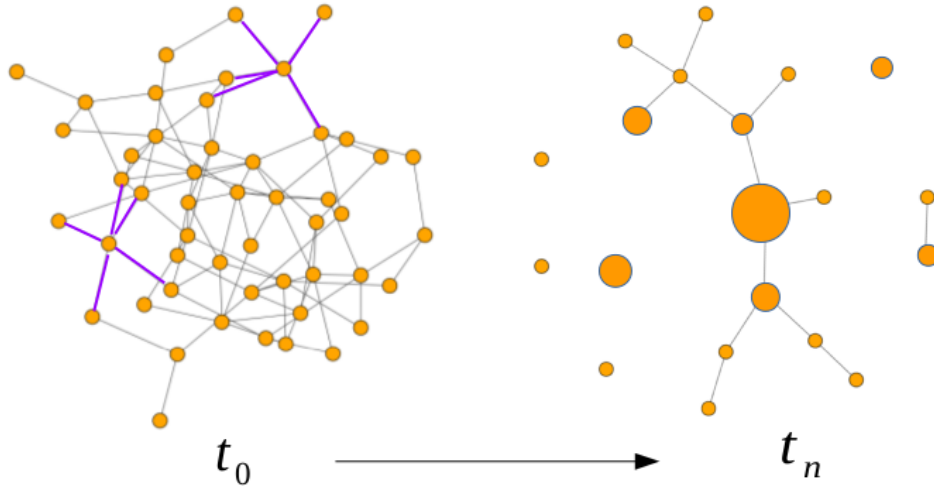


Figure 2.11: *The Erdős-Rényi random network (ER), generated with $\langle k \rangle = 4$, at t_0 the beginning of the game, and after n time steps. Only nodes with wealth are shown on the figure, while the size of the nodes indicates their accumulated wealth.*

means there is no direct link between them at the start of the game. Our hypothesis leads to the fact that the average number of remaining nodes is roughly equal to the ensemble averaged number of nodes that aren't first order neighbors. We can calculate the approximate average number of remaining nodes from sampling on all configurations of nodes that are not connected with each other. The detailed calculations are described in the thesis, but in the end we arrive at a value for the number of remaining nodes N_R :

$$N_R \approx N_0 \frac{1 + \frac{\langle k \rangle - 2}{\langle k \rangle} \ln \left(\frac{\langle k \rangle}{2} - 1 \right)}{\frac{3}{2} \langle k \rangle - 2} \quad (2.12)$$

where N_0 is the initial number of nodes and k is the degree of the graph, $\langle k \rangle = pN_0$. The average wealth, $\langle w \rangle$ of the N_R remaining nodes is then:

$$\langle w \rangle = \frac{N_0 w_0}{N_R} \approx \frac{N_0 w_0}{N_p} = w_0 \frac{\frac{3}{2} \langle k \rangle - 2}{1 + \frac{\langle k \rangle - 2}{\langle k \rangle} \ln \left(\frac{\langle k \rangle}{2} - 1 \right)} \quad (2.13)$$

We then assume that all distributions of the remaining wealth in the system are equally probable, which leads us to exponential distribution for wealth in the final state:

$$\rho(w) \approx \alpha e^{-\alpha w}, \quad (2.14)$$

with $\alpha = 1/\langle w \rangle$. By taking into account the fact that there must only be one node with

maximum wealth in the final distribution, we can calculate the maximum wealth value:

$$w_{max} = w_0 \frac{N_0}{N_R} \ln(N_R) \quad (2.15)$$

In order to obtain the expression for the expected duration of the game we need to determine the most probable time for reaching this threshold, assuming a simple Brownian motion approximation for the wealth with steps of one unit wealth.

By taking a look at first passage time of a random walk [10], we can estimate the duration of the game as

$$\tau \approx \frac{1}{3} w_{max}^2 \quad (2.16)$$

Taking into account our estimate for w_{max} we get

$$\tau \approx \frac{w_0^2}{3} \left[\frac{N_0}{N_R} \ln(N_R) \right]^2 \quad (2.17)$$

leading to:

$$\tau^{1/2} \approx \frac{w_0}{\sqrt{3}} \frac{\frac{3}{2}\langle k \rangle - 2}{1 + \frac{\langle k \rangle - 2}{\langle k \rangle} \ln\left(\frac{\langle k \rangle}{2} - 1\right)} \left[\ln(N_0) + \ln\left(\frac{1 + \frac{\langle k \rangle - 2}{\langle k \rangle} \ln\left(\frac{\langle k \rangle}{2} - 1\right)}{\frac{3}{2}\langle k \rangle - 2}\right) \right] \quad (2.18)$$

This results suggests that $\tau^{1/2}$ scales linearly with the initial wealth (w_0) and it has a linear dependence as a function of the logarithm of the graphs size ($\ln N_0$). The dependence as a function of the average connectivity of the graph is more complex.

Another approach is to study the coarse-grained dynamics of the system's variables by tracing their connections with each other and their evolution in time.

The most important characteristics of the system are the number of active nodes $N(t)$ (with non-zero wealth and connected to other non-zero nodes) and the number of active connections $N_c(t)$. We will also introduce the following variables: N_0 , which is the initial number of nodes, $N_i(t)$, the number of nodes that have wealth, but are isolated, and $N_n(t)$, nodes that do not have wealth (naturally: $N(t) + N_i(t) + N_n(t) = N_0$).

Taking into consideration the connection between the number of active nodes and active connections, we can write:

$$\frac{dN_c}{dt} = -c(t) \frac{dN_n}{dt} = c(t) \frac{dN}{dt} \quad (2.19)$$

where $c(t) = \frac{2N_c(t)}{N(t)}$ is the average number of active connections per node at time t . As with the previous approach, we can treat each individual node's wealth as a random walk, and we assume that the time to run out of wealth is the most probable first passage time [10]:

$$\tau = w^2(t)/3, \quad (2.20)$$

This is the time in which the number of nodes without wealth increases by one unit. The time unit was fixed in our model as $N_c(0) = L$ trials on all the links of the $G(N, p)$

ER, graph. The probability to hit an active connection, while selecting the $N_c(0)$ links is: $N_c(t)/N_c(0)$. According to these, we can approximate the rate at which the number of nodes without wealth increases:

$$\frac{dN_n}{dt} = \frac{3}{w^2(t)} \frac{N_c(t)}{N_c(0)} N_c(0) = N_c(t) \frac{3}{w^2(t)} \quad (2.21)$$

Since we neglected the isolated nodes in our approximation, the average wealth of the active nodes is easily computable:

$$w(t) \approx \frac{N_0 w_0}{N(t)} \quad (2.22)$$

We have thus two coupled differential equations for describing the dynamics of the system:

$$\begin{aligned} \frac{dN_c}{dt} &= \frac{2N_c(t)}{N(t)} \frac{dN}{dt} \\ \frac{dN}{dt} &= -\frac{3N(t)^2}{N_0^2 w_0^2} N_c(t) \end{aligned} \quad (2.23)$$

which leads to:

$$N_c(t) = L \left[\frac{9tL}{N_0 w_0^2} + 1 \right]^{-2/3} = \langle k \rangle N_0 \left[\frac{9t\langle k \rangle}{w_0^2} + 1 \right]^{-2/3} \quad (2.24)$$

This dynamic approach, although is valid at the beginning and middle of the game, does not give us a good approximation of the duration of the game, as the error becomes too big as time increases. So, in order to find the final state of the system, we will use the results of the final state approximation and compare them with computer simulations.

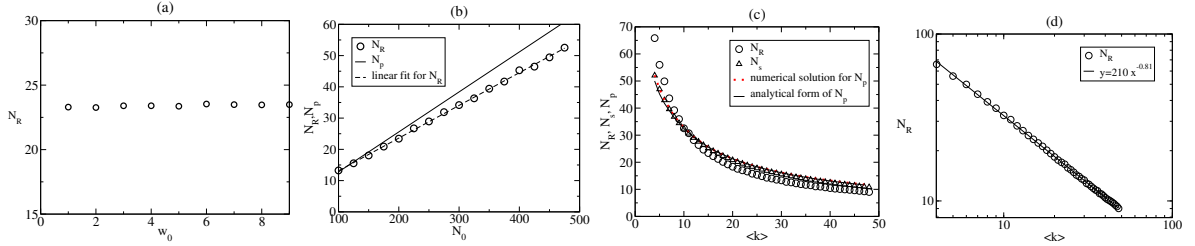


Figure 2.12: Simulation results for the average number of remaining nodes. (a) Results as a function of the initial wealth of the nodes, w_0 ($\langle k \rangle = 15$ and $N_0 = 200$); (b) Results as a function of the initial size of the graph, N_0 . The continuous line indicates the N_p value given by equation (2.12) and with dashed line we indicate the best linear fit for the simulation results. ($\langle k \rangle = 15$, $w_0 = 4$); (c) Results as function of the average number of links per node, $\langle k \rangle$. The circles, dotted line and continuous line indicate the simulation results obtained by different approximations. ($N_0 = 200$, $w_0 = 4$); (d) Power-law fit for the simulation results presented in figure (c). Please note the logarithmic axes.

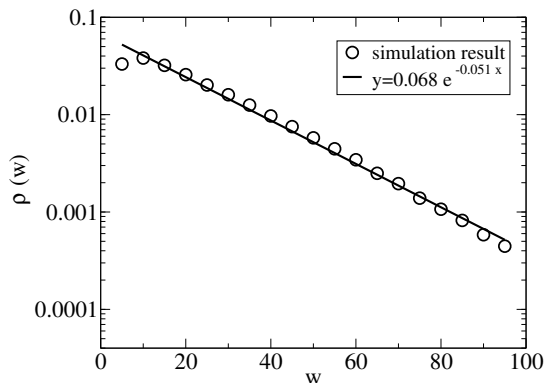


Figure 2.13: *Exponential distribution of wealth for the nodes that remain with finite wealth at the end of the game. Please note the logarithmic axis for $\rho(w)$. Circles are simulation results, while the continuous line is an exponential fit: $\rho(w) = 0.068 \cdot \exp(-0.051w)$. ($N_0 = 200$, $\langle k \rangle = 10$ and $w_0 = 4$).*

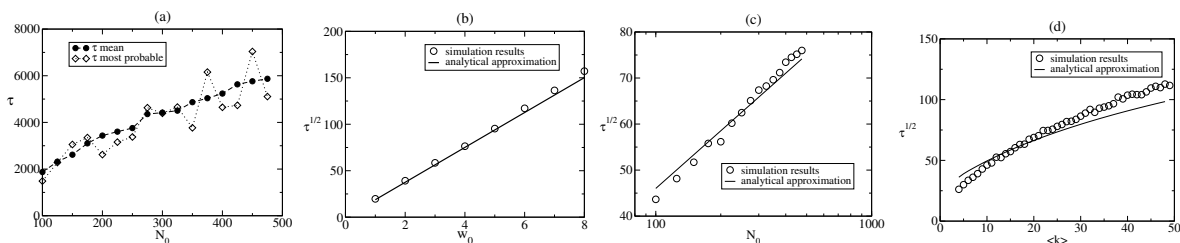


Figure 2.14: *Simulation results for the time-length of the ruin game. (a) Comparison between the mean and most probable length of the game. ($\langle k \rangle = 15$ and $w_0 = 4$); (b) Square root for the games time-length as a function of the nodes initial wealth w_0 (circles) ($\langle k \rangle = 15$ and $N_0 = 500$); (c) Square root of game length as a function of the initial size of the graph, N_0 (circles). ($\langle k \rangle = 15$ and $w_0 = 4$). Please notice the logarithmic axis for N_0 ; (d) Square root of the games length as a function of the mean degree of the nodes, $\langle k \rangle$. ($w_0 = 4$ and $N_0 = 200$). For figures (b), (c) and (d) the continuous line indicates our analytical approximation (2.18).*

The validity of our assumptions and approximations can be verified by means of a Monte Carlo simulation of the system. We generate an Erdős-Rényi graph and simulate every time step of our ruin game, then average the results over up to 10000 trials. Figure 2.12 shows that the simulation results are very close to our analytical solutions for the number of remaining nodes. The assumption of exponential distribution of wealth in remaining nodes is confirmed by simulations as well (fig. 2.13). Figures 2.14 and 2.15 demonstrate the validity of the approximation for the game duration, as well as the fact that most probable duration coincides with the average duration.

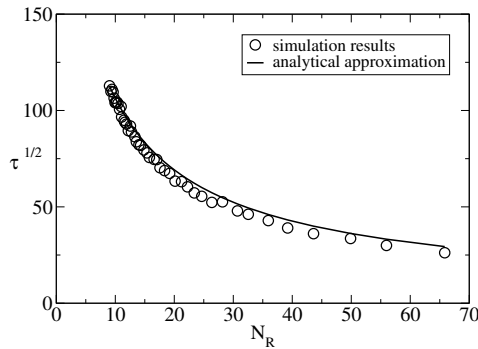


Figure 2.15: *Square root for the game length as a function of the number of nodes with nonzero wealth in the final configuration. Circles are simulation results both for τ and N_R , while the continuous line is given by equation (2.17). ($N_0 = 200$, $w_0 = 4$ and $\langle k \rangle \in [4, 50]$).*

2.5 Conclusions

We have studied several systems of varying complexity that display spontaneous self-organization and found the conditions for phase transitions in all of them. In systems of coupled oscillators we found temporal patterns that exist only in specific regions of the parameter space, such as full synchronization, anti-phase synchronization and quasi-periodic oscillations. In the ruin game, we found spatial patterns that manifest themselves in specific numbers of nodes that retain wealth at the end, exponential distribution of wealth among them, independent of the particular graph's topology.

These findings are general enough to be observed in equivalent systems of biological, physical or electronic nature, and perhaps someday can help in understanding, predicting, and modeling the behavior of real world self-organizing systems, like multi-cellular organisms, neural networks, behaviors of animal colonies, and many others.

3 Scientific contributions

Publications related to the thesis:

1. Néda, Z., Davidova, L., Újvári, S. and Istrate, G., 2017. Gambler's ruin problem on Erdős Rényi graphs. *Physica A: Statistical Mechanics and its Applications*, 468, pp.147-157.

I've programmed the computer simulations in the work and derived the equations for the time-evolution approach to the system. I also contributed to editing and writing the manuscript.

2. Davidova, L., Borbély, S. and Néda, Z., 2015. Collective Behavior of Coupled Quantum Mechanical Oscillators. *Studia Universitatis Babeş-Bolyai, Physica*, 60(1).

I came up with the idea to study this system and did all the work on programming and analyzing the results.

3. Davidova, L., Boda, Sz. and Néda, Z., 2014. Order-disorder Transitions in a Minimal Model of Self-sustained Coupled Oscillators. *Romanian Reports in Physics*, 66(4), pp.1018-1028.

I've conducted a lot of computer simulations on the system of coupled oscillators and discovered potentially new effects of synchronization as a function of the system parameters.

4. Boda, S., Davidova, L. and Néda, Z., 2014. Order and disorder in coupled metronome systems. *The European Physical Journal Special Topics*, 223(4), pp.649-663.

I've contributed with suggestions that certain system parameters can have interesting effects on the dynamics of the system and helped on computer simulations.

5. Davidova, L., Újvári, Sz. and Néda, Z., 2014. Sync or anti-sync – dynamical pattern selection in coupled self-sustained oscillator systems. In *Journal of Physics: Conference Series* (Vol. 510, No. 1, p. 012009). IOP Publishing.

All of the computer simulations in the work were done by me, as well as the analysis of the results.

Conference participation:

1. 25th IUPAP Conference on Computational Physics (CCP2013) – Poster Presentation

2. 14th International Balkan Workshop on Applied Physics (IBWAP 2014) – Poster Presentation
3. IV Summer School on Statistical Physics of Complex and Small Systems – Poster Presentation

Bibliography

- [1] C Huygens. Letter to de sluse, in: Oeuvres completes de christian huygens.
- [2] Matthew Bennett, Michael F Schatz, Heidi Rockwood, and Kurt Wiesenfeld. Huygens's clocks. *Proceedings: Mathematics, Physical and Engineering Sciences*, pages 563–579, 2002.
- [3] Krzysztof Czołczynski, Przemysław Perlikowski, Andrzej Stefanski, and Tomasz Kapitaniak. Huygens'odd sympathy experiment revisited. *International Journal of Bifurcation and Chaos*, 21(07):2047–2056, 2011.
- [4] James Pantaleone. Synchronization of metronomes. *American Journal of Physics*, 70(10):992–1000, 2002.
- [5] Sz Boda, Zoltan Neda, Botond Tyukodi, and Arthur Tunyagi. The rhythm of coupled metronomes. *The European Physical Journal B*, 86(6):1–9, 2013.
- [6] Sz Boda, L Davidova, and Z Néda. Order and disorder in coupled metronome systems. *The European Physical Journal Special Topics*, 223(4):649–663, 2014.
- [7] Henning Ulrichs, Andreas Mann, and Ulrich Parlitz. Synchronization and chaotic dynamics of coupled mechanical metronomes. *Chaos: An Interdisciplinary Journal of Nonlinear Science*, 19(4):043120, 2009.
- [8] GW Ford, M Kac, and P Mazur. Statistical mechanics of assemblies of coupled oscillators. *Journal of Mathematical Physics*, 6(4):504–515, 1965.
- [9] Gian Luca Giorgi, Fernando Galve, Gonzalo Manzano, Pere Colet, and Roberta Zambrini. Quantum correlations and mutual synchronization. *Physical Review A*, 85(5):052101, 2012.
- [10] Geoffrey R Grimmett and David R Stirzaker. *Probability and Random Process*. Oxford University Press, New York, 2001.